Exploiting Power Adaptation With Transmit Antenna Selection for Interference-Outage Constrained Underlay Spectrum Sharing

Rimalapudi Sarvendranath, *Student Member, IEEE*, and Neelesh B. Mehta, *Fellow, IEEE*

***Abstract*— In underlay spectrum sharing, the interference constraint limits transmissions by the secondary transmitter, which concurrently accesses the spectrum, to protect the primary user from excessive interference. Transmit antenna selection enables a secondary user to overcome the limitations imposed by the interference constraint using low-complexity hardware. We develop an optimal and novel joint antenna selection and power adaptation rule that minimizes the average symbol error probability (SEP) of a secondary user that is subject to two practically well-motivated constraints. The first is the less-studied but general interference-outage constraint, which limits the probability that the interference power at the primary receiver exceeds a threshold. The second constraint limits the peak transmit power of the secondary transmitter. We show that the optimal rule for the interference-outage constraint has a novel structure that is markedly different from the rules considered in the literature. We then present an insightful geometric interpretation of its structure. Using this, we also propose a practically amenable and near-optimal variant of the optimal rule called the linear rule, and analyze its performance. Our numerical results show that the optimal rule reduces the average SEP by one to two orders of magnitude compared to the rules in the literature.**

***Index Terms*— Spectrum sharing, underlay, antenna selection, power adaptation, interference outage.**

I. Introduction

THE demand for high wireless data rates, which require large amounts of wireless spectrum, has seen a tremendous increase over the years. However, enough bandwidth is not available for the upcoming wireless technologies in the sub-6 GHz bands, which have favorable propagation characteristics [2], [3]. To address this pressing issue, the regulatory authorities are now releasing spectrum bands for shared and unlicensed operations [4], [5]. For example, the Federal Communications Commission has opened up 1.2 GHz of spectrum in the 6 GHz band in USA [5], which is currently occupied by the primary users (PUs) such as satellite services, to be shared by unlicensed secondary users (SUs) such as 5G new radio (NR) unlicensed and IEEE 802.11ax/be [3]. Other wireless standards such as the citizen's broadband radio service and MulteFire are also based on the coexistence of new SUs with the existing PUs [6]. These SUs can reuse the spectrum so long as they do not cause excessive interference to the existing PUs. The interference constraint, which effectively specifies what 'excessive' means, plays a key role in driving the transmission strategy of the SU and its performance.

In underlay spectrum sharing, an SU transmits even when the PU is using the spectrum but is subject to constraints on the interference it causes to the primary receiver (PRx). It is appealing because it improves the spectrum utilization significantly and is practically feasible [7]. While these interference constraints protect the PU from interference, they can significantly limit the SU's performance [8]. To overcome these challenges, low hardware complexity multiple antenna techniques such as hybrid precoding [9], spatial modulation [10], and antenna selection [8], [11] have been studied. In hybrid precoding, the secondary transmitter (STx) transmits a signal that is combined in the digital domain and in the analog domain [12]. Whereas, spatial modulation selects an antenna based on the symbol to be transmitted [13]. In transmit antenna selection (TAS), which is the focus of this paper, the STx dynamically selects one among multiple antennas depending on the instantaneous channel state, connects it to the single available radio frequency (RF) chain, and transmits data to the secondary receiver (SRx) [14]. This switching happens once in a coherence interval [14]. It improves the SU's performance with a hardware complexity comparable to a single antenna system [8], [15]–[18].

In conventional interference-unconstrained systems, the antenna selected and the transmit power depend only on the channel gains between the transmitter and the receiver [19]. However, antenna selection and power adaptation (ASPA) in an underlay spectrum sharing system must also consider the STx to PRx (STx-PRx) channel gains because it needs to simultaneously control the interference at the PRx. Consider, for example, the peak interference constraint, which limits the instantaneous interference power at the PRx [17], [18]. In [17], the transmit antenna with the smallest STx-PRx channel power gain is selected. In [18], the antenna with the highest ratio of the STx to SRx (STx-SRx) channel power gain and STx-PRx channel power gain is instead selected.

Manuscript received April 22, 2019; revised September 12, 2019; accepted October 21, 2019. Date of publication October 31, 2019; date of current version January 15, 2020. This work was supported in part by the Kaikini Ph.D. Scholarship in Engineering and the DST-Swarnajayanti Fellowship award DST/SJF/ETA-01/2014-15. This article was presented in part at the IEEE Global Communcations Conference (Globecom), December 2019 [1]. The associate editor coordinating the review of this article and approving it for publication was M. Abdallah. *(Corresponding author: Rimalapudi Sarvendranath.)*

The authors are with the Department of Electrical Communication Engineering, Indian Institute of Science (IISc), Bengaluru 560012, India (e-mail: sarvendranath@gmail.com; nbmehta@iisc.ac.in).

Digital Object Identifier 10.1109/TCOMM.2019.2950680

In both these references the transmit power of the STx is inversely proportional to the STx-PRx channel power gain of the selected antenna.

The ASPA rules turn out to be very different for stochastic constraints such as the average interference constraint [20], which limits the fading-averaged interference power at the PRx, and the interference-outage constraint [21], which limits the probability that the instantaneous interference power at the PRx exceeds a threshold. We discuss them in more detail below.

1) *Average Interference Constraint:* For an STx that transmits with peak power or with zero power, which we refer to as *on-off* power adaptation, the optimal rule that minimizes the symbol error probability (SEP) selects the antenna that minimizes a net cost that is a linear function of the STx-PRx channel power gain and an exponentially decreasing function of the STx-PRx channel power gain [22]. However, for an STx that varies the transmit power as a continuous function of the channel power gains, which we refer to as *continuous* power adaptation, the optimal rule selects the antenna that maximizes the ratio of the STx-SRx channel power gain and an affine function of the STx-PRx channel power gain [20].
2) *Interference-Outage Constraint:* For on-off power adaptation, the SEP-optimal antenna minimizes a net cost that is a discontinuous function of the STx-PRx channel power gain [21]. It is unlike any of the aforementioned rules. However, the optimal ASPA rule for continuous power adaptation is not known in the literature.

A. Focus and Contributions

In this paper, we consider an underlay secondary system that is subject to the interference-outage constraint. While the model of an STx transmitting to an SRx and causing interference to a PRx has been studied in the literature, key questions remain open. Firstly, which interference constraint to impose and what its parameters should be are still open questions for the spectrum regulators and standards bodies. Though the peak interference constraint has been well studied in the literature [15]–[18], the implications of stochastic constraints such as the interference-outage constraint on the secondary system are not well understood. A change in something as fundamental as the interference constraint leads to a different optimization problem and a different optimal solution [16], [21], [22]. Secondly, optimal continuous power adaptation with TAS for the interference-outage constraint is not well understood.

We make the following contributions:

1) *Optimal Rule:* We present a novel optimal TAS and continuous power adaptation rule that minimizes the average SEP, which is an important measure of the reliability of communication [16], [18], [23], of an interference-outage and peak transmit power constrained underlay secondary system. It applies to a general class of fading channel models with a continuous cumulative distribution function (CDF), which includes the widely studied Rayleigh, Rician, and Nakagami-m models.

   Continuous power adaptation provides more flexibility to an STx in controlling its transmit power while requiring the same channel state information (CSI) as on-off power adaptation. The interference-outage constraint is a generalization of the conservative peak interference constraint [15]–[18]. Given its stochastic nature, it is suitable for practical scenarios with imperfect CSI at the STx, unlike the peak interference constraint [21], [24]. Moreover, it is suitable for primary systems that offer delay or disruption-tolerant services and are designed to tolerate outages due to co-channel interference [21], [23].
2) *Geometric Characterization and Linear Rule:* The optimal rule assigns a transmit power and net cost to each antenna and selects the antenna with the lowest net cost. We present an insightful geometric characterization of the optimal transmit power and the net cost as a function of the STx-SRx and STx-PRx channel power gains. We exploit it to develop a new and simpler rule called the linear rule.
3) *Performance Analysis:* We derive bounds for the average SEP and the interference-outage probability of the linear rule that apply to any fading model with a continuous CDF. The interference-outage bound yields a computationally-simpler way to implement the linear rule in practice. We show that these expressions simplify considerably in the asymptotic regime of large transmit power.
4) *Benchmarking and Impact of Imperfect CSI:* Our numerical results show that the optimal rule can achieve a one to two orders of magnitude lower SEP than the rules considered in the literature [16]–[18], [21]. They also show that imperfect STx-SRx CSI and imperfect STx-PRx CSI have different impacts on the average SEP and the interference-outage probability.

We note that our derivation of the optimal ASPA rule for the interference-outage constraint is different from the ones for the peak interference constraint [16]–[18] or the average interference constraint [20], [22]. It applies to all fading models with a continuous CDF. It is more involved and different from that for on-off power adaptation in [21]. Also, the structure of the optimal rule cannot be inferred from the above ASPA rules. For example, for the peak interference constraint, the transmit power is independent of the STx-SRx channel power gain [16]–[18], while for the average interference constraint, it is a continuous function of the ratio of the STx-SRx and STx-PRx channel power gains [20]. On the other hand, the transmit power of our ASPA rule is a discontinuous function of both STx-SRx and STx-PRx channel power gains. Consequently, its average SEP and interference-outage probability analysis turns out to be very different. Moreover, the impact of imperfect CSI with continuous power adaptation is different from that in [21], while [20], [22] consider only perfect CSI.

B. Outline and Notation

Section II presents the system model and the problem statement. The optimal ASPA rule is derived in Section III.

The linear rule is developed and analyzed in Section IV. Performance benchmarking and numerical results are presented in Section V. Our conclusions follow in Section VI.

Notation: Scalar variables are written in normal font, vector variables in bold font, and sets in calligraphic font. The probability of an event A and the conditional probability of A given B are denoted by $\Pr(A)$ and $\Pr(A|B)$, respectively. $\mathbb{E}_X[\cdot]$ denotes expectation with respect to a random variable (RV) X. The $\mathcal{O}(\cdot)$ notation is as per the Bachmann-Landau notation [25, Chap. 3]. The null set is denoted by $\varnothing$. And, $I_{\{a\}}$ denotes the indicator function; it is 1 if a is true and is 0 otherwise.

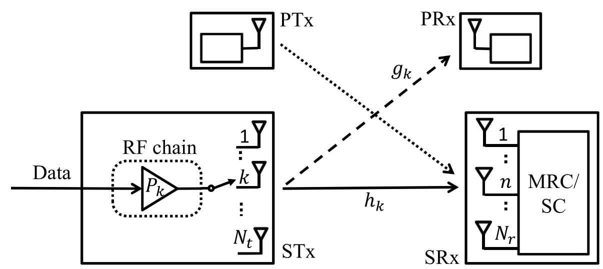

Fig. 1. System model that consists of an STx with N_t transmit antennas and one RF chain. It transmits data to an SRx with N_r antennas, which causes interference to a PRx.

II. System Model and Problem Statement

The system model is shown in Figure 1. It consists of an STx that communicates with an SRx, and, in the process, interferes with a PRx that is equipped with a single antenna. The STx dynamically selects one among N_t transmit antennas and connects it to the single RF chain that is available [14], [19]. The SRx is equipped with N_r antennas and employs either maximal ratio combining (MRC) or selection combining (SC) [26]. The instantaneous channel power gain from the k^{th} antenna of the STx to the n^{th} antenna of the SRx is denoted by h_{nk}, and the instantaneous channel power gain from the k^{th} antenna of the STx to the PRx is denoted by g_k. We assume that the STx-SRx channel gains are independent and identically distributed (i.i.d.) RVs, and so are the STx-PRx channel gains [8], [16]–[18].

The instantaneous SEP when the STx transmits using antenna k with power P_k is denoted by $\mathsf{S}(P_k, h_k)$. It is given by [26, (9.7)], [21]

$$\mathsf{S}(P_k, h_k) \approx c_1 \exp\left(-c_2 \frac{P_k h_k}{\sigma^2}\right), \text{ for } 1 \le k \le N_t, \quad (1)$$

where c_1 and c_2 are modulation-dependent parameters, and $\sigma^2 = \sigma_t^2 + \sigma_i^2$ is the sum of thermal noise power σ_t^2 and the interference power σ_i^2 at the SRx due to transmissions from the primary transmitter (PTx).[1] Here, $h_k = \max_{1 \le n \le N_r}\{h_{nk}\}$ for SC and $h_k = \sum_{n=1}^{N_r} h_{nk}$ for MRC. Let $\mathbf{h} \triangleq [h_1, \ldots, h_{N_t}]$ and $\mathbf{g} \triangleq [g_1, \ldots, g_{N_t}]$.

CSI Model: Our CSI model, which is similar to those in [16]–[18], [20], [21], is as follows:

i) *STx:* It knows the STx-SRx channel power gains $\mathbf{h}$ and the STx-PRx channel power gains $\mathbf{g}$. It does not need the phase information of any of these channel gains. When the secondary and primary systems operate in the time division duplexing mode, it can obtain $\mathbf{h}$ and $\mathbf{g}$ by making use of reciprocity [28]. However, when they operate in the frequency division duplexing mode, it can obtain $\mathbf{h}$ using feedback and $\mathbf{g}$ using a hidden power-feedback loop technique [29]. Other techniques to obtain $\mathbf{g}$ are summarized in [30].

ii) *SRx:* It performs coherent demodulation. For this, it needs to know only the complex baseband channel gains from the transmit antenna selected by the STx to itself. This can be estimated using the pilot symbols embedded with the data.

A. Constraints and Problem Statement

An ASPA rule ϕ is a mapping from $(\mathbb{R}^+)^{N_t} \times (\mathbb{R}^+)^{N_t}$ to $\{1, 2, \ldots, N_t\} \times [0, P_{\max}]$. It maps $(\mathbf{h}, \mathbf{g})$ to the selected antenna $s \in \{1, 2, \ldots, N_t\}$ and the transmit power $P_s \in [0, P_{\max}]$.

The STx is subject to the following two constraints:

1) *Interference-Outage Constraint [21], [23]:* The instantaneous interference power at the PRx is equal to $P_s g_s$. An interference-outage happens when $P_s g_s > \tau$, where τ is the interference power threshold. The interference-outage constraint can be stated as

$$\Pr(P_s g_s > \tau) \le O_{\max}, \quad (2)$$

where $O_{\max}$ is the maximum allowed for the interference-outage. The probability distributions of $\mathbf{h}$ and $\mathbf{g}$ and the ASPA rule together determine this probability.

2) *Peak Transmit Power Constraint [15], [16]:* This limits P_s to be less than or equal to a peak transmit power $P_{\max}$.

Our goal is to derive an optimal rule ϕ^* that minimizes the average SEP of the secondary system that is subject to the above two constraints. Our problem can be mathematically stated as the following stochastically constrained optimization problem $\mathcal{P}$:

$$\mathcal{P}: \quad \min_{\phi} \ \mathbb{E}_{\mathbf{h},\mathbf{g}}\left[\mathsf{S}(P_s, h_s)\right], \quad (3)$$

$$\text{s.t. } \Pr(P_s g_s > \tau) \le O_{\max}, \quad (4)$$

$$0 \le P_s \le P_{\max}, \quad (5)$$

$$(s, P_s) = \phi(\mathbf{h}, \mathbf{g}). \quad (6)$$

III. Optimal Rule and its Behavior

A. Optimal Rule

First, consider the interference-outage unconstrained scenario. Since the instantaneous SEP is a monotonically decreasing function of $P_s h_s$, it is easy to see that the optimal rule should select the antenna with the highest STx-SRx channel power gain and transmit with power $P_{\max}$. We shall

[1] Implicit in this summation and (1) is the assumption that the interference is Gaussian. This assumption is physically justified by the central limit theorem when there are multiple PTxs and is valid even with one PTx if it uses a constant amplitude signal [23]. This assumption is widely used in the literature due to its tractability [20], [22], [23], [27].

refer to this as the *unconstrained* (UC) rule. It can be written as

$$s = \underset{k \in \{1,2,\ldots,N_t\}}{\arg\max} \{h_k\} \text{ and } P_s = P_{\max}. \tag{7}$$

Its interference-outage probability $O_u(\tau)$ is

$$O_u(\tau) \triangleq \Pr(P_{\max} g_s > \tau). \tag{8}$$

Since the antenna selected by the UC rule is independent of $\mathbf{g}$ and $g_1, \ldots, g_{N_t}$ are i.i.d., it follows that

$$O_u(\tau) = \Pr(P_{\max} g_1 > \tau) = F_g^c(\tau / P_{\max}), \tag{9}$$

where $F_g^c(\cdot)$ denotes the complementary CDF of the identically distributed RVs $g_1, \ldots, g_{N_t}$.

When $O_u(\tau) \le O_{\max}$, which we shall refer as the *unconstrained regime*, the UC rule satisfies the constraint in (4) and is optimal. However, when $O_u(\tau) > O_{\max}$, which we shall refer to as the *constrained regime*, the UC rule does not satisfy the interference-outage constraint. It, thus, cannot solve $\mathcal{P}$. We now develop the optimal rule for this regime using the following three lemmas. Lemma 1 shows that selecting an antenna and transmit power that minimizes an instantaneous net cost (defined below) is optimal provided a penalty factor $\lambda^* > 0$ exists such that the interference-outage constraint is met with equality. Lemma 2 presents a closed-form expression for the transmit power of an antenna if it were selected to transmit. Lemma 3 proves that the penalty factor λ^* does indeed exist and is unique.

Lemma 1: In the constrained regime, the following ASPA rule $(s^*, P_{s^*}) = \phi^*(\mathbf{h}, \mathbf{g})$ is optimal:

$$(s^*, P_{s^*}) \triangleq \underset{\{(k,P_k)\ :\ k=\{1,2,\ldots,N_t\},\ P_k \in [0,P_{\max}]\}}{\arg\min} \{\mathsf{NC}_k\}, \tag{10}$$

where the net cost NC_k of antenna k is given by

$$\mathsf{NC}_k \triangleq \mathsf{S}(P_k, h_k) + \lambda I_{\{P_k g_k > \tau\}}. \tag{11}$$

This holds provided that the penalty factor $\lambda > 0$ can be set to λ^* such that the interference-outage probability is equal to $O_{\max}$, i.e., $\Pr(P_{s^*} g_{s^*} > \tau) = O_{\max}$.

Proof: The proof is given in Appendix A. ■

Lemma 2: For antenna k, the transmit power P_k that minimizes its net cost NC_k is given by

$$P_k = \begin{cases} P_{\max}, & \text{if } P_{\max} g_k \le \tau, \\ P_{\max}, & \text{if } \mathsf{S}\left(\frac{\tau}{g_k}, h_k\right) > \mathsf{S}(P_{\max}, h_k) + \lambda, \\ \frac{\tau}{g_k}, & \text{else.} \end{cases} \tag{12}$$

Proof: The proof is given in Appendix B. ■

These two lemmas imply that for every antenna k, the optimal rule first computes the value of P_k in (12) and substitutes this in (11). It then selects the antenna with the smallest net cost.

Lemma 3: For any fading model with a continuous CDF and $0 < O_{\max} < O_u(\tau)$, a unique $\lambda^* \in (0, c_1)$ always exists such that $\Pr(P_{s^*} g_{s^*} > \tau) = O_{\max}$.

Proof: The proof is given in Appendix C. ■

Here, the optimal penalty factor λ^* has to be computed numerically, which is typical in several constrained optimization problems [26], [27]. In Section IV, we shall present a simpler ASPA rule and a computationally simpler way of determining its penalty factor. The above approach can be generalized to optimize other performance metrics such as ergodic rate and rate-outage probability, but the optimal rules so obtained will be different.

B. Behavior of the Optimal Rule

A key insight from (12) is that the transmit power P_k and the net cost NC_k of antenna k take different values in the following three mutually exclusive regions of (h_k, g_k):

1) If an antenna k belongs to the region
$$\mathcal{U}_k = \{(h_k, g_k) : P_{\max} g_k \le \tau\}, \tag{13}$$
it transmits with peak power, i.e., $P_k = P_{\max}$, and does not cause an interference-outage. Hence, we shall call it an *outage-compliant peak power* (OCPP) antenna. Its net cost is $\mathsf{NC}_k = \mathsf{S}(P_{\max}, h_k)$.
2) If an antenna k belongs to the region
$$\mathcal{C}_k = \{(h_k, g_k) : P_{\max} g_k > \tau, \\ \mathsf{S}(\tau/g_k, h_k) \le \mathsf{S}(P_{\max}, h_k) + \lambda\}, \tag{14}$$
it transmits with power $P_k = \tau / g_k < P_{\max}$ and does not cause an interference-outage. Hence, we shall call it an *outage-compliant power constrained* (OCPC) antenna. Its net cost is $\mathsf{NC}_k = \mathsf{S}(\tau/g_k, h_k)$.
3) If an antenna k belongs to the region
$$\mathcal{I}_k = \{(h_k, g_k) : \mathsf{S}(\tau/g_k, h_k) > \mathsf{S}(P_{\max}, h_k) + \lambda\}, \tag{15}$$
it again transmits with $P_{\max}$ but it causes an interference-outage because $P_{\max} g_k > \tau$. Hence, we shall call it an *outage-inducing* (OI) antenna. Its net cost is $\mathsf{NC}_k = \mathsf{S}(P_{\max}, h_k) + \lambda$. We see here that λ is the penalty of an OI antenna for causing an interference-outage.

The three regions are shown in Figure 2a. The behavior of the optimal rule depends on λ as follows:

1) $\lambda = 0$: From (14) and (15), we get $\mathcal{C}_k = \varnothing$ and $\mathcal{I}_k = \{(h_k, g_k) : P_{\max} g_k > \tau\}$. Hence, $P_k = P_{\max}$, for all $k \in \{1, 2, \ldots, N_t\}$, and the optimal rule reduces to the UC rule in (7).
2) $0 < \lambda < c_1$: The optimal rule causes an interference-outage only if it selects an OI antenna. It transmits with the peak power $P_{\max}$ only if it selects an OCPP antenna or an OI antenna.
3) $\lambda = c_1$: Here, $\mathcal{I}_k = \varnothing$ and $\mathcal{C}_k = \{(h_k, g_k) : P_{\max} g_k > \tau\}$ because $\mathsf{S}(\tau/g_k, h_k) \le c_1$. Hence, $P_k = P_{\max}$ for $P_{\max} g_k \le \tau$, and $P_k = \tau / g_k$, otherwise. Since $P_k g_k \le \tau$, for all k, and the SEP is a monotonically decreasing function of $P_k h_k$, the optimal rule reduces to $s^* = \arg\max_{1 \le k \le N_t} \{P_k h_k\}$. This is equivalent to the rule specified in [16].

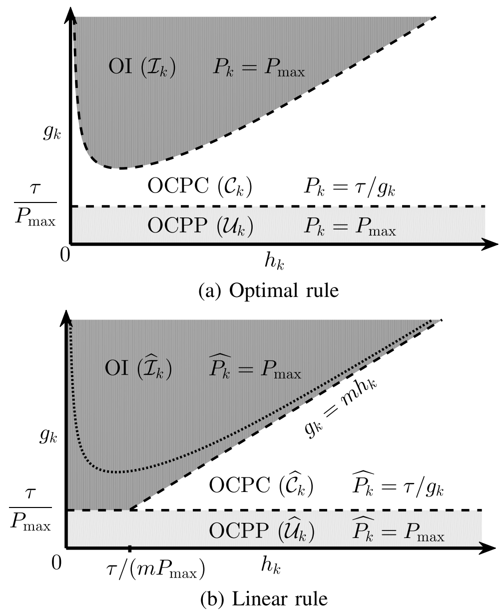

Fig. 2. Illustrations of the OCPP, OCPC, and OI regions and transmit power of antenna k in them as a function of h_k and g_k.

IV. Simpler Linear Rule, Analysis, and Insights

The involved form of the boundary of the OCPC and OI regions in the optimal rule and the numerical search needed to determine λ^* motivate the simpler linear rule that we present below.

Based on Section III-B, we first specify the linear rule in terms of its corresponding three regions OCPP ($\widehat{\mathcal{U}}_k$), OCPC ($\widehat{\mathcal{C}}_k$), and OI ($\widehat{\mathcal{I}}_k$) for any antenna k. We obtain $\widehat{\mathcal{C}}_k$ and $\widehat{\mathcal{I}}_k$ by dropping the $\mathsf{S}\left(P_{\max}, h_k\right)$ term in the inequalities in (14) and (15), respectively, and set $\widehat{\mathcal{U}}_k = \mathcal{U}_k$. The rationale behind this will become clear when we analyze the linear rule. Using (1) and algebraic simplifications, the three regions for this rule can be written as

$$\text{OCPP}: \widehat{\mathcal{U}}_k = \left\{(h_k, g_k) : P_{\max} g_k \leq \tau\right\}, \tag{16a}$$
$$\text{OCPC}: \widehat{\mathcal{C}}_k = \left\{(h_k, g_k) : P_{\max} g_k > \tau, g_k \leq m h_k\right\}, \tag{16b}$$
$$\text{OI}: \widehat{\mathcal{I}}_k = \left\{(h_k, g_k) : P_{\max} g_k > \tau, g_k > m h_k\right\}, \tag{16c}$$

where

$$m \triangleq \frac{-c_2 \tau}{\sigma^2 \ln\left(\lambda / c_1\right)}, \quad \text{for } \lambda \in (0, c_1), \tag{17}$$

is the slope of the line that divides the OCPC and OI regions. This is illustrated in Figure 2b. For $\lambda = 0$, $m \triangleq 0$ and for $\lambda = c_1$, $m \triangleq \infty$.

Linear Rule Specification: In terms of the above three regions, the linear rule can be specified as follows. It first computes the power $\widehat{P}_k$ of antenna k as follows:

$$\widehat{P}_k = \begin{cases} \frac{\tau}{g_k}, & \text{if } (h_k, g_k) \in \widehat{\mathcal{C}}_k, \\ P_{\max}, & \text{else.} \end{cases} \tag{18}$$

It then selects the antenna $s = \arg\min_{1 \leq k \leq N_t} \left\{\widehat{\mathsf{NC}}_k\right\}$, where

$$\widehat{\mathsf{NC}}_k \triangleq \mathsf{S}(\widehat{P}_k, h_k) + \lambda I_{\left\{\widehat{P}_k g_k > \tau\right\}}, \text{ for } 1 \leq k \leq N_t, \tag{19}$$

and transmits with power $\widehat{P}_s$.

The relationship between the linear and optimal rules depends on λ as explained below:

- $\lambda = 0$: Here, the inequality $g_k > m h_k$ in (16c), which is equivalent to $\mathsf{S}\left(\tau/g_k, h_k\right) > \lambda = 0$, is always true. Substituting this in (16b) and (16c) yields $\widehat{\mathcal{C}}_k = \varnothing$ and $\widehat{\mathcal{I}}_k = \left\{(h_k, g_k) : P_{\max} g_k > \tau\right\}$. From Section III-B, we can see that $\widehat{\mathcal{C}}_k = \mathcal{C}_k$ and $\widehat{\mathcal{I}}_k = \mathcal{I}_k$. Thus, the linear rule becomes equivalent to the optimal rule.
- $0 < \lambda < c_1$: The difference between the OCPC and OI regions of the linear and optimal rules decreases as $P_{\max}$ increases since the term $\mathsf{S}\left(P_{\max}, h_k\right)$, which is dropped to obtain $\widehat{\mathcal{C}}_k$ and $\widehat{\mathcal{I}}_k$, is an exponentially decreasing function of $P_{\max}$. Thus, the linear rule becomes closer to the optimal rule as $P_{\max}$ increases.
- $\lambda = c_1$: As above for $\lambda = 0$, we can again show that the linear rule is equivalent to the optimal rule.

Result 1: Given λ, the average SEP of the linear rule lower bounds that of the optimal rule.

Proof: The proof is given in Appendix D. ■

Note: For a given λ, the interference-outage probabilities of the two rules are different. In fact, the interference-outage probability of the linear rule upper bounds that of the optimal rule. Our model, ASPA rules, and analysis can be extended to a system with multiple antennas at the PRx by constraining the outage probability of the total interference power at the PRx. The optimal and linear rules are obtained by replacing g_s with the sum of channel power gains from the STx antenna s to all the antennas at the PRx.

A. Performance Analysis

We now derive general bounds for the average SEP and the interference-outage probability O_λ of the linear rule that apply to any fading model and any value of N_t and N_r. Let $\mathbb{E}\left[h_{nk}\right] = \mu_h$ and $\mathbb{E}\left[g_k\right] = \mu_g$. Let $\Omega = P_{\max}\mu_h/\sigma^2$ denote the peak fading-averaged signal-to-interference-plus-noise ratio (SINR) at the SRx. Let

$$\beta_m = \frac{\tau}{m P_{\max}},$$

denote the value of h_k where the line $g_k = m h_k$ intersects the horizontal line $g_k = \tau/P_{\max}$. Let $\widehat{U}_k \triangleq \{(h_k, g_k) \in \widehat{\mathcal{U}}_k\}$, $\widehat{C}_k \triangleq \{(h_k, g_k) \in \widehat{\mathcal{C}}_k\}$, and $\widehat{I}_k \triangleq \{(h_k, g_k) \in \widehat{\mathcal{I}}_k\}$ denote the events in which (h_k, g_k) belongs to the OCPP, OCPC, and OI regions, respectively.

1) Average SEP $\left(\overline{\mathsf{SEP}}\right)$*:* Let E denote the error event. Then, $\overline{\mathsf{SEP}}$ is given by

$$\overline{\mathsf{SEP}} = \mathbb{E}_{\mathbf{h},\mathbf{g}}\left[\Pr\left(\mathrm{E}|\mathbf{h},\mathbf{g}\right)\right] = N_t \mathbb{E}_{\mathbf{h},\mathbf{g}}\left[\Pr\left(s = 1, \mathrm{E}|\mathbf{h},\mathbf{g}\right)\right], \tag{20}$$

where the second equality follows by symmetry. Using the law of total probability, we have

$$\Pr\left(s = 1, \mathrm{E}|\mathbf{h},\mathbf{g}\right) = \sum_{R \in \left\{\widehat{U}_1, \widehat{C}_1, \widehat{I}_1\right\}} \Pr\left(s = 1, R, \mathrm{E}|\mathbf{h},\mathbf{g}\right). \tag{21}$$

Using the chain rule, we get $\Pr\left(s = 1, R, \mathrm{E}|\mathbf{h},\mathbf{g}\right) = (s = 1, R|\mathbf{h},\mathbf{g}) \Pr\left(\mathrm{E}|s = 1, R, \mathbf{h},\mathbf{g}\right)$, for $R \in \left\{\widehat{U}_1, \widehat{C}_1, \widehat{I}_1\right\}$.

Substituting the transmit power in each of the regions as per (18), we get

$$\begin{aligned}\Pr(s=1,\mathsf{E}|\mathbf{h},\mathbf{g}) = & \Pr\left(s=1,\widehat{U}_1|\mathbf{h},\mathbf{g}\right)\mathsf{S}(P_{\max},h_1)\\ & +\Pr\left(s=1,\widehat{C}_1|\mathbf{h},\mathbf{g}\right)\mathsf{S}(\tau/g_1,h_1)\\ & +\Pr\left(s=1,\widehat{I}_1|\mathbf{h},\mathbf{g}\right)\mathsf{S}(P_{\max},h_1).\end{aligned} \quad (22)$$

Substituting (22) in (20) and using the law of total expectation, we get

$$\overline{\mathsf{SEP}} = T_{\text{OCPP}} + T_{\text{OCPC}} + T_{\text{OI}}, \quad (23)$$

where

$$T_{\text{OCPP}} = N_t \mathbb{E}_{h_1}\left[\Pr\left(s=1,\widehat{U}_1|h_1\right)\mathsf{S}(P_{\max},h_1)\right], \quad (24)$$

$$T_{\text{OCPC}} = N_t \mathbb{E}_{h_1,g_1}\left[\Pr\left(s=1,\widehat{C}_1|h_1,g_1\right)\mathsf{S}(\tau/g_1,h_1)\right], \quad (25)$$

$$T_{\text{OI}} = N_t \mathbb{E}_{h_1}\left[\Pr\left(s=1,\widehat{I}_1|h_1\right)\mathsf{S}(P_{\max},h_1)\right]. \quad (26)$$

The above terms T_{OCPP}, T_{OCPC}, and T_{OI} correspond to the average SEPs due to the OCPP, OCPC, and OI regions, respectively. We simplify these terms using the four lemmas below. Lemmas 4 and 5 deal with T_{OCPP}, Lemma 6 with T_{OCPC}, and Lemma 7 with T_{OI}.

Lemma 4: The conditional probability of $s=1$ and antenna 1 being in $\widehat{\mathcal{U}}_1$ given h_1 equals

$$\begin{aligned}\Pr\left(s=1,\widehat{U}_1|h_1\right) = & (1-O_u(\tau))\left[T_{\text{uu}}(h_1)+T_{\text{uc}}(h_1)\right.\\ & \left.+T_{\text{ui}}(h_1)\right]^{N_t-1}, \end{aligned}\quad (27)$$

where

$$\begin{aligned}T_{\text{uu}}(h_1) &= \Pr\left(h_2 < h_1, \widehat{U}_2\right),\\ T_{\text{uc}}(h_1) &= \Pr\left((\tau h_2/g_2) < P_{\max}h_1, \widehat{C}_2\right),\\ T_{\text{ui}}(h_1) &= \Pr\left(\mathsf{S}(P_{\max},h_2)+\lambda > \mathsf{S}(P_{\max},h_1), \widehat{I}_2\right).\end{aligned}$$

Proof: The proof is given in Appendix E. ■

Lemma 4 leads to the following upper bound for T_{OCPP}.

Lemma 5: The average SEP due to the OCPP region is bounded as $T_{\text{OCPP}} \le B_{\text{OCPP}}$, where

$$\begin{aligned}B_{\text{OCPP}} = & N_t(1-O_u(\tau))\int_0^{\beta_m}\left[(1-O_u(\tau))F_h(h_1)\right.\\ & \left.+O_u(\tau)F_h(\omega(h_1))\right]^{N_t-1}\mathsf{S}(P_{\max},h_1)f_h(h_1)\,dh_1\\ & +N_t(1-O_u(\tau))\int_{\beta_m}^{\infty}\left[(1-O_u(\tau))F_h(h_1)\right.\\ & \left.+O_u(\tau)\right]^{N_t-1}\mathsf{S}(P_{\max},h_1)f_h(h_1)\,dh_1, \end{aligned}\quad (28)$$

where $F_h(\cdot)$ and $f_h(\cdot)$ denote the CDF and probability density function (PDF), respectively, of the i.i.d. RVs $h_1,\ldots,h_{N_t}$, and $\omega(h_1) \triangleq -\sigma^2\ln\left(e^{-\frac{c_2 P_{\max}}{\sigma^2}h_1} - \frac{\lambda}{c_1}\right)/(c_2 P_{\max})$.

Proof: The proof is given in Appendix F. ■

For example, for Rayleigh fading and MRC, we have

$$F_h(x) = 1 - e^{-\frac{x}{\mu_h}}\sum_{n=0}^{N_r-1}\frac{1}{n!}\left(\frac{x}{\mu_h}\right)^n, \quad \text{for } x\in[0,\infty).$$

And, for Rayleigh fading and SC, we have

$$F_h(x) = \left(1-e^{-\frac{x}{\mu_h}}\right)^{N_r}, \text{ for } x\in[0,\infty).$$

In a similar manner, we can show the following for the OCPC region:

$$\begin{aligned}\Pr\left(s=1,\widehat{C}_1|h_1,g_1\right) = & I_{\{P_{\max}g_1>\tau, g_1\le m h_1\}}\left[T_{\text{cu}}(h_1,g_1)\right.\\ & \left.+T_{\text{cc}}(h_1,g_1)+T_{\text{ci}}(h_1,g_1)\right]^{N_t-1}, \end{aligned}\quad (29)$$

where

$$T_{\text{cu}}(h_1,g_1) = \Pr\left(P_{\max}h_2 < \frac{\tau h_1}{g_1}, \widehat{U}_2\right), \quad (30)$$

$$T_{\text{cc}}(h_1,g_1) = \Pr\left(\frac{h_2}{g_2} < \frac{h_1}{g_1}, \widehat{C}_2\right), \quad (31)$$

$$T_{\text{ci}}(h_1,g_1) = \Pr\left(\mathsf{S}(P_{\max},h_2)+\lambda > \mathsf{S}(\tau/g_1,h_1), \widehat{I}_2\right). \quad (32)$$

This leads to the following expression for T_{OCPC}.

Lemma 6: The average SEP of the OCPC region can be simplified as follows:

$$\begin{aligned}T_{\text{OCPC}} = & N_t\int_{\frac{\tau}{P_{\max}}}^{\infty}\int_{\frac{g_1}{m}}^{\infty}\left[\Omega(h_1,g_1)\right]^{N_t-1}\mathsf{S}(\tau/g_1,h_1)\\ & \times f_h(h_1)\,f_g(g_1)\,dh_1\,dg_1, \end{aligned}\quad (33)$$

where $\Omega(h_1,g_1) \triangleq F_h(\tau h_1/(P_{\max}g_1))(1-O_u(\tau)) + \int_{\tau/P_{\max}}^{\infty}F_h(h_1 x/g_1)\,f_g(x)\,dx$.

Proof: The proof is given in Appendix G. ■

Lastly, in the OI region, we can show that

$$\begin{aligned}\Pr\left(s=1,\widehat{I}_1|h_1\right) = & \Pr\left(\widehat{I}_1|h_1\right)\left[T_{\text{iu}}(h_1)+T_{\text{ic}}(h_1)\right.\\ & \left.+T_{\text{ii}}(h_1)\right]^{N_t-1}, \end{aligned}\quad (34)$$

where

$$T_{\text{iu}}(h_1) = \Pr\left(\mathsf{S}(P_{\max},h_2) > \mathsf{S}(P_{\max},h_1)+\lambda, \widehat{U}_2\right), \quad (35)$$

$$T_{\text{ic}}(h_1) = \Pr\left(\mathsf{S}(\tau/g_2,h_2) > \mathsf{S}(P_{\max},h_1)+\lambda, \widehat{C}_2\right), \quad (36)$$

$$T_{\text{ii}}(h_1) = \Pr\left(h_2 < h_1, \widehat{I}_2\right). \quad (37)$$

This leads to the following upper bound for T_{OI}.

Lemma 7: The average SEP from the OI region is bounded as $T_{\text{OI}} \le B_{\text{OI}}$, where

$$\begin{aligned}B_{\text{OI}} = & N_t\int_0^{\beta_m}O_u(\tau)\left[F_h(h_1)\right]^{N_t-1}\mathsf{S}(P_{\max},h_1)\\ & \times f_h(h_1)\,dh_1\\ & +N_t\int_{\beta_m}^{\infty}F_g^c(mh_1)\left[F_h(\beta_m)+\Psi(\beta_m)\right]^{N_t-1}\\ & \times\mathsf{S}(P_{\max},h_1)\,f_h(h_1)\,dh_1, \end{aligned}\quad (38)$$

where $\Psi(\beta_m) = \int_{\beta_m}^{\infty}F_g^c(mx)\,f_h(x)\,dx$.

Proof: The proof is given in Appendix H. ■

Combining (28), (33), and (38) yields following general upper bound for the average SEP:

$$\overline{\mathsf{SEP}} \le B_{\text{OCPP}} + T_{\text{OCPC}} + B_{\text{OI}}. \quad (39)$$

Behavior of Average SEP: i) As $P_{\max}$ increases, T_{OCPP} decreases because the OCPP region $\widehat{\mathcal{U}}_k$ (cf. (16a)) shrinks and $\mathsf{S}\left(P_{\max}, h_k\right)$ decreases. T_{OCPC} increases for small $P_{\max}$ and saturates for large $P_{\max}$ because the OCPC region $\widehat{\mathcal{C}}_k$ (cf. (16b)) increases for small $P_{\max}$ and then saturates. T_{OI} increases for small $P_{\max}$ and then decreases. ii) As τ increases, T_{OCPP} increases because the OCPP region $\widehat{\mathcal{U}}_k$ (cf. (16a)) increases. T_{OCPC} decreases because $\mathsf{S}\left(\tau/g_1, h_1\right)$ decreases exponentially. T_{OI} decreases slowly for small τ but decreases faster for large τ.

To gain more insights, consider Rayleigh fading and $N_r = 1$. In this case, the expression for B_{OCPP} in (28) reduces to

$$\begin{aligned} B_{\text{OCPP}} = N_t c_1 &\sum_{\substack{j\geq 0, k\geq 0, n\geq 0,\\ j+k+n=N_t-1}} \frac{(N_t-1)!}{j!k!n!} \frac{\left(1-O_u\left(\tau\right)\right)^{j+1}}{O_u\left(\tau\right)^{-k}} \\ &\times \sum_{l=0}^{\infty} \frac{(-1)^{j+k+l}\left(\frac{\lambda}{c_1}\right)^l \left(1-\left(\frac{\lambda}{c_1}\right)^{\frac{j+k+1}{c_2\Omega}+1-l}\right)}{l!\left(j+k+1+c_2\Omega(1-l)\right)} \\ &\times \frac{\Gamma\left(\frac{k}{c_2\Omega}+1\right)}{\Gamma\left(\frac{k}{c_2\Omega}-l+1\right)} + N_t c_1 \sum_{k=0}^{N_t-1} \binom{N_t-1}{k} \\ &\times \frac{(-1)^k \left(1-O_u\left(\tau\right)\right)^{k+1}}{k+1+c_2\Omega} \left(\frac{\lambda}{c_1}\right)^{\frac{k+1}{c_2\Omega}+1}. \end{aligned} \tag{40}$$

T_{OCPC} in (33) reduces to

$$\begin{aligned} T_{\text{OCPC}} = \frac{N_t c_1}{\mu_g \mu_h} &\int_{\frac{\tau}{P_{\max}}}^{\infty} \int_{\frac{g_1}{m}}^{\infty} \exp\left(-\frac{c_2\tau}{\sigma^2}\frac{h_1}{g_1} - \frac{h_1}{\mu_h} - \frac{g_1}{\mu_g}\right) \\ &\times \Bigg[1-(1-O_u\left(\tau\right))e^{-\frac{\tau}{P_{\max}\mu_h}\frac{h_1}{g_1}} \\ &- \frac{O_u\left(\tau\right)\mu_h g_1}{\mu_h g_1 + \mu_g h_1} e^{-\frac{\tau}{P_{\max}\mu_h}\frac{h_1}{g_1}}\Bigg]^{N_t-1} dh_1 dg_1. \end{aligned} \tag{41}$$

This can be further simplified by using the inequality $(1+x)^{-1} \geq e^{-x}$, for $x \geq 0$, to bound $\left(1+\mu_g h_1/(\mu_h g_1)\right)^{-1}$. Doing so yields $T_{\text{OCPC}} \leq B_{\text{OCPC}}$, where

$$\begin{aligned} B_{\text{OCPC}} = N_t c_1 &\sum_{\substack{j\geq 0, k\geq 0, n\geq 0,\\ j+k+n=N_t-1}} \frac{(N_t-1)!}{j!k!n!} (-1)^{j+k} \left(1-O_u\left(\tau\right)\right)^k \\ &\times \left(\frac{O_u\left(\tau\right)^{j+1+\frac{\mu_g}{m\mu_h}}}{1+\frac{\mu_g}{m\mu_h}} \left(\frac{\lambda}{c_1}\right)^{\frac{j+k}{c_2\Omega}+\frac{j\mu_g\sigma^2}{\mu_h c_2 \tau}+1} \right. \\ &- \left[\frac{(j+k+c_2\Omega)\tau}{\mu_g P_{\max}} + j\right] O_u\left(\tau\right)^{-k-c_2\Omega} e^j \\ &\left. \times E_1\left[\left(\frac{(j+k+1+c_2\Omega)\tau}{\mu_g P_{\max}} + j\right)\alpha\right]\right), \end{aligned} \tag{42}$$

where $\alpha = 1 + m\mu_h/\mu_g$ and $E_1\left[z\right] = \int_z^{\infty}\left(e^{-t}/t\right)dt$ is the exponential integral [31, pp. xxxv]. Similarly, B_{OI} in (38) reduces to

$$\begin{aligned} B_{\text{OI}} = &\frac{N_t c_1 \mu_g}{c_2\Omega\mu_g + m\mu_h + \mu_g} \left(\frac{\lambda}{c_1}\right)^{\frac{1}{c_2\Omega}+1} \\ &\times \left[1-\left(\frac{\lambda}{c_1}\right)^{\frac{1}{c_2\Omega}} + \frac{O_u\left(\tau\right)\mu_g}{\mu_g + m\mu_h}\left(\frac{\lambda}{c_1}\right)^{\frac{1}{c_2\Omega}}\right]^{N_t-1} \\ &+ \sum_{k=0}^{N_t-1} \binom{N_t-1}{k} \frac{(-1)^k N_t c_1 O_u\left(\tau\right)}{k+1+c_2\Omega} \\ &\times \left(1-\left(\frac{\lambda}{c_1}\right)^{\frac{k+1}{c_2\Omega}+1}\right). \end{aligned} \tag{43}$$

Combining (40), (42), and (43) yields the following closed-form upper bound:

$$\overline{\mathsf{SEP}} \leq B_{\text{OCPP}} + B_{\text{OCPC}} + B_{\text{OI}}. \tag{44}$$

2) Interference-Outage Probability:

Result 2: The interference-outage probability O_λ is bounded as $O_\lambda \leq B_\lambda$, where

$$B_\lambda = \left[F_h\left(\beta_m\right) + \Psi\left(\beta_m\right)\right]^{N_t} - \left(1-O_u\left(\tau\right)\right)\left[F_h\left(\beta_m\right)\right]^{N_t}. \tag{45}$$

Proof: The proof is given in Appendix I. ■

Practical Implications: Consider the linear rule whose penalty factor λ is obtained by solving $B_\lambda = O_{\max}$. It satisfies the interference-outage constraint since $B_\lambda \geq O_\lambda$. This is much simpler than solving the equation $O_\lambda = O_{\max}$ and makes it easy to implement the linear rule. We will see in Section V that this leads to a negligible degradation in the SEP.

To gain more insights, consider the example of Rayleigh fading with SC. In this case, (45) simplifies to the following closed-form expression:

$$\begin{aligned} B_\lambda = &\left(\sum_{n=0}^{N_r-1}\binom{N_r-1}{n}\frac{(-1)^n N_r O_u\left(\tau\right)\mu_g}{(n+1)\mu_g + m\mu_h}\left(\frac{\lambda}{c_1}\right)^{\frac{n+1}{c_2\Omega}} \right. \\ &\left. + \Lambda^{N_r}\right)^{N_t} - \left(1-O_u\left(\tau\right)\right)\Lambda^{N_t N_r}, \end{aligned} \tag{46}$$

where $\Lambda = 1 - \left(\lambda/c_1\right)^{\frac{1}{c_2\Omega}}$.

B. Asymptotic Behavior and Insights for Large P_{max}

As mentioned, the linear and optimal rules become equivalent to each other for large $P_{\max}$. Specifically, the three regions reduce to $\mathcal{U}_k = \widehat{\mathcal{U}}_k \to \varnothing$, $\mathcal{C}_k = \widehat{\mathcal{C}}_k \to \{(h_k, g_k) : g_k \leq m h_k\}$, and $\mathcal{I}_k = \widehat{\mathcal{I}}_k \to \{(h_k, g_k) : g_k > m h_k\}$.

Interference-Outage Probability: From (18) and (19), for an OCPC antenna, we have $\widehat{P}_k = \tau/g_k$ and $\widehat{\mathsf{NC}}_k = \mathsf{S}\left(\tau/g_k, h_k\right)$. From the definition of the slope m in (17), the inequality $g_k \leq m h_k$ can be written as $\mathsf{S}\left(\tau/g_k, h_k\right) \leq \lambda \leq \mathsf{S}\left(P_{\max}, h_k\right) + \lambda$. Similarly, for an OI antenna, we have $\widehat{P}_k = P_{\max}$ and $\widehat{\mathsf{NC}}_k = \mathsf{S}\left(P_{\max}, h_k\right) + \lambda \geq \mathsf{S}\left(\tau/g_k, h_k\right)$. Thus, an OI antenna is selected only if all the antennas are in the OI region. Since an interference-outage happens only when an OI antenna is selected, we get

$O_\lambda = \Pr(g_1 > mh_1, g_2 > mh_2, \ldots, g_{N_t} > mh_{N_t})$. Since the channel power gains are i.i.d., it follows that

$$O_\lambda = [\Pr(g_1 > mh_1)]^{N_t} = \left[\int_0^\infty F_g^c(mh_1) f_h(h_1)\, dh_1\right]^{N_t}. \quad (47)$$

For example, for Rayleigh fading and SC, (47) simplifies to

$$O_\lambda = \left[\sum_{n=0}^{N_r-1} \binom{N_r-1}{n} \frac{(-1)^n N_r \mu_g}{(n+1)\mu_g + m\mu_h}\right]^{N_t}. \quad (48)$$

For $N_r = 1$, equating this with $O_{\max}$ yields the following exact closed-form expression for λ:

$$\lambda = c_1 \exp\left(-\frac{c_2 \tau \mu_h}{\sigma^2 \mu_g} \frac{(O_{\max})^{1/N_t}}{(1-(O_{\max})^{1/N_t})}\right). \quad (49)$$

This brings out how λ depends on $O_{\max}$, τ, and N_t.

Average SEP: For large $P_{\max}$, $\mathsf{S}(P_{\max}, h_k) \to 0$. Thus, in (23), $T_{\mathrm{OCPP}} \to 0$, $T_{\mathrm{OI}} \to 0$, and $\overline{\mathsf{SEP}} = T_{\mathrm{OCPC}}$. Substituting $P_{\max} \to \infty$ in (33) yields

$$\overline{\mathsf{SEP}} = N_t \int_0^\infty \int_{\frac{g_1}{m}}^\infty \left[\int_0^\infty F_h\left(\frac{h_1}{g_1}x\right) f_g(x)\, dx\right]^{N_t-1} \times \mathsf{S}\left(\frac{\tau}{g_1}, h_1\right) f_h(h_1) f_g(g_1)\, dh_1\, dg_1. \quad (50)$$

For example, for Rayleigh fading with $N_t = 2$ and $N_r = 1$, the above expression simplifies to

$$\overline{\mathsf{SEP}} = (2 + c_2 a)\left(\lambda b - c_1 c_2 a e^{c_2 a} E_1\left[\frac{c_2 a}{b}\right]\right) - \lambda b^2, \quad (51)$$

where $a = \tau\mu_h/(\sigma^2\mu_g)$ and $b = 1 - \sqrt{O_{\max}}$.

V. Numerical Results and Performance Benchmarking

We compare the performance of the optimal and linear rules with the following ASPA rules: minimum interference rule [17], maximum ratio rule [18], and maximum signal power rule [16]. As originally proposed, these rules set the transmit power as $P_k = \min\{P_{\max}, \tau/g_k\}$. This leads to an interference-outage probability of zero. In order to enable them to take advantage of the non-zero interference-outage probability $O_{\max}$ that is allowed, we generalize them using the following probabilistic transmit power policy: $P_k = P_{\max}$ if $P_{\max} g_k \le \tau$; else,

$$P_k = \begin{cases} P_{\max}, & \text{with probability } q, \\ \frac{\tau}{g_k}, & \text{with probability } 1-q, \end{cases} \quad (52)$$

where $q > 0$ is numerically set such that the interference-outage probability is equal to $O_{\max}$.

The minimum interference rule selects the antenna $s = \arg\min_{1 \le k \le N_t}\{g_k\}$ and its transmit power P_s is as per (52). The maximum ratio rule selects the antenna $s = \arg\max_{1 \le k \le N_t}\{h_k/g_k\}$ and its transmit power P_s is as per (52). The maximum signal power rule first computes P_k as per (52) for each antenna k. It then selects the antenna $s = \arg\max_{1 \le k \le N_t}\{P_k h_k\}$ and transmits with power P_s. In addition, to evaluate the gains from continuous power adaptation, we also compare with the *on-off* rule [21] that selects one among the N_t antennas and whose transmit power is either $P_{\max}$ or 0. The latter is denoted by $s = 0$ with $h_0 \triangleq 0$ and $g_0 \triangleq 0$. It selects the antennas as follows:

$$s = \underset{k \in \{0,1,\ldots,N_t\}}{\arg\min} \left\{\mathsf{S}(P_{\max}, h_k) + \alpha I_{\{P_{\max} g_k > \tau\}}\right\}, \quad (53)$$

where α is chosen such that $\Pr(P_s g_s > \tau) = O_{\max}$ in the constrained regime. Else, $\alpha = 0$.

We show results for Rayleigh fading and set $\mu_h = -114$ dB, $\mu_g = -121$ dB, and $\sigma_t^2 = -114$ dBm. The ratio of the interference power at the SRx to the thermal noise power is 2.2; hence, $\sigma^2 = \sigma_t^2 + \sigma_i^2 = -109$ dBm. The peak fading-averaged SINR $\Omega = P_{\max}\mu_h/\sigma^2$ is 10 dB for $P_{\max} = 15$ dBm.[2] We use $(c_1, c_2) = (0.5, 0.6)$ for QPSK [32, (13)], $(c_1, c_2) = (0.6, 0.18)$ for 8-PSK, and $(c_1, c_2) = (0.8, 0.12)$ for 16-QAM.[3] The simulation curves in all the figures are based on symbol-level simulations and do not use the SEP formula in (1).

Figure 3 benchmarks the average SEP of the optimal rule and the linear rule with the above ASPA rules. They behave differently in the following two regimes: (i) *Unconstrained regime* ($\Omega \le 2.9$ dB): Here, the optimal rule, the linear rule, the maximum signal power rule, and the on-off rule are the same as the UC rule. Hence, their SEPs are the same and they decrease as Ω increases. (ii) *Constrained regime* ($\Omega > 2.9$ dB)[4]: Here, the penalty factor of each rule is chosen such that its interference-outage probability is equal to $O_{\max}$. The SEPs of all the rules decrease as Ω increases and reach error floors. This is because, for large Ω, the SEP is negligible when the STx transmits with power $P_{\max}$. It is dominated by the event in which the STx transmits with power τ/g_k. The error floor of the optimal rule is lower by a factor of 5.7, 5.7, 87.8, and 107.6 than that of the maximum signal power, maximum ratio, minimum interference rules, and optimal TAS rule with on-off power adaptation, respectively. Thus, the optimal rule exploits the available CSI much more effectively. We also see that the linear rule is near-optimal. This shows that dropping $\mathsf{S}(P_{\max}, h_k)$ in its design (cf. Section IV) makes a negligible difference.

Figure 4 plots the average SEP of the linear rule as a function of the normalized interference power threshold τ/σ^2 for two constellations and for different values of N_t and N_r. We compare its performance when the penalty factor λ is obtained by equating the exact interference-outage probability O_λ to $O_{\max}$ and when it is obtained by equating the interference-outage upper bound B_λ in (45) to $O_{\max}$. We see that the difference in the average SEPs obtained using O_λ and using B_λ is negligible. Thus, the linear rule can be implemented in a near-optimal manner with a lower complexity. In the *constrained regime* ($\tau/\sigma^2 < 7.1$ dB, $\lambda > 0$),

[2]This corresponds to a carrier frequency of 2.4 GHz, bandwidth of 1 MHz, 300 K noise temperature, path-loss exponent of 3.7, reference distance of 1 m, a distance of 100 m between the STx and SRx, and a distance of 150 m between the STx and PRx for the simplified path-loss model [26, Chap. 2.6].

[3]The values for 8-PSK and 16-QAM are obtained by accurate curve-fitting; the other values have been used in [16], [18].

[4]From (9), we can show that the constrained regime corresponds to $\Omega > -\tau\mu_h/(\mu_g\sigma^2 \ln(O_{\max}))$, in general.

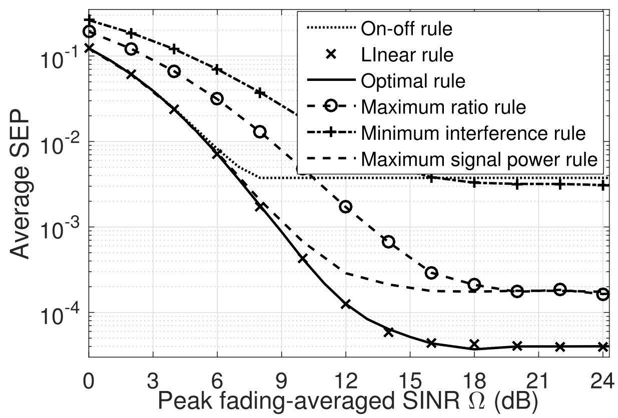

Fig. 3. Performance benchmarking: Average SEP as a function of Ω for different ASPA rules ($O_{\max} = 0.01$, $\tau/\sigma^2 = 3$ dB, $N_t = 4$, $N_r = 2$, SC, and QPSK).

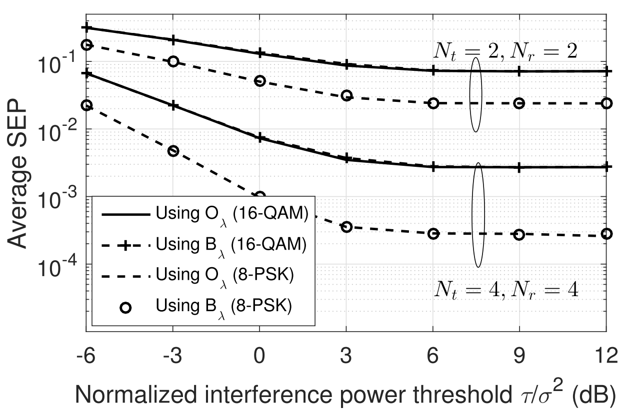

Fig. 4. Linear rule: Average SEP as a function of τ/σ^2 ($O_{\max} = 0.1$, $\Omega = 10$ dB, and MRC).

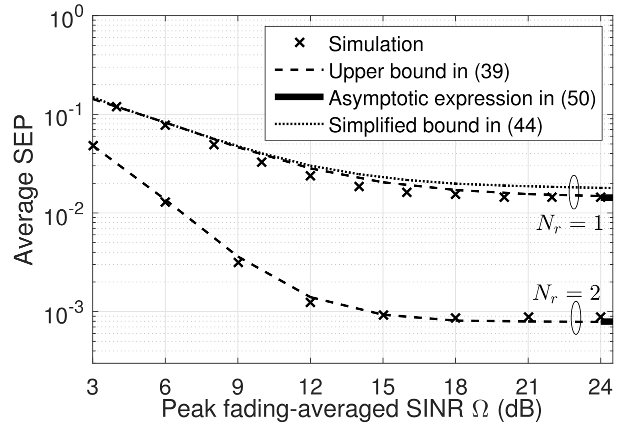

Fig. 5. Linear rule: Average SEP and its bound as a function of Ω for different values of N_r ($O_{\max} = 0.1$, $\tau/\sigma^2 = 0$ dB, $N_t = 2$, MRC, and QPSK).

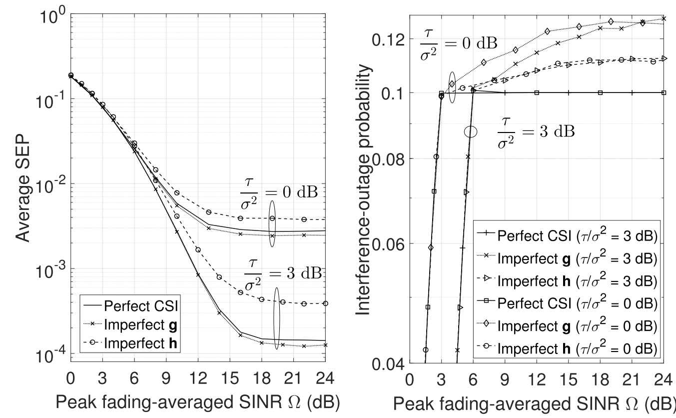

(a) Average SEP (b) Interfernece-outage probability

Fig. 6. Impact of imperfect CSI on average SEP and interference-outage probability as a function of Ω ($O_{\max} = 0.1$, $N_t = 2$, $N_r = 2$, SC, and QPSK).

the average SEP decreases as τ increases. This is because the STx transmits with a higher power since the instantaneous interference power allowed is higher. In the *unconstrained regime* ($\tau/\sigma^2 \geq 7.1$ dB, $\lambda = 0$), the average SEP reaches a floor. This is because the linear rule becomes equivalent to the UC rule, whose SEP is independent of τ. We also see that the error floor decreases significantly as N_t or N_r increases.

Figure 5 plots the average SEP of the linear rule as a function of Ω for different values of N_r. In the constrained regime, the penalty factor λ is chosen such that the exact interference-outage probability O_λ is equal to $O_{\max}$. Also shown are the general upper bound and asymptotic expressions in (39) and (50), respectively, for both N_r values. We see that this bound is tight for all Ω.[5] We also see that the closed-form upper bound in (44) for $N_r = 1$ tracks the simulation curve well.

Impact of Imperfect CSI at the STx: We now present separate results for imperfect estimates of $\mathbf{h}$ and $\mathbf{g}$ to understand their impacts. They are obtained by the STx from corresponding pilots using minimum mean square error channel estimation [21], [23], [24]. The pilot SNR is set to 15 dB. As before, the secondary receiver SRx knows the complex channel gain of the selected STx-SRx link perfectly.

Figures 6a and 6b plot the average SEP and the interference-outage probability, respectively, of the optimal rule with imperfect CSI for two value of τ. Consider first $\tau/\sigma^2 = 0$ dB. Here, the system is in the unconstrained regime for $\Omega \leq 3$ dB. Therefore, the transmit antenna selected is independent of $\mathbf{g}$ (cf. (7)) and the interference-outage probability is equal to $O_u(\tau)$ even with imperfect CSI; it increases as Ω increases. The impact of imperfect CSI on the average SEP is also negligible. The behavior is different in the constrained regime ($\Omega > 3$ dB). Now, the interference-outage constraint is violated due to imperfect CSI. With imperfect $\mathbf{g}$, this happens because the STx transmits with a higher power more often. Consequently, the average SEP decreases compared to the perfect CSI case. With imperfect $\mathbf{h}$, the interference-outage probability again exceeds $O_{\max}$, but by a smaller value. However, the average SEP degrades more and reaches a higher floor. For $\tau/\sigma^2 = 3$ dB, the system transitions to the constrained regime at $\Omega = 6$ dB. The trends in the SEP are similar to those above, except that the error

[5]For $\Omega \geq 18$ dB, the simulation results of $N_r = 2$ case marginally exceed the bound. This is because of the approximate nature of the SEP expression in (1).

floors are lower. However, the interference-outage probability becomes the same as for $\tau/\sigma^2 = 0$ dB for large Ω.

VI. Conclusion

We developed a novel SEP-optimal joint ASPA rule for an interference-outage and peak transmit power constrained secondary system. We saw that the net cost, which the rule strove to minimize, and the optimal transmit power of each antenna were discontinuous functions of both STx-SRx and STx-PRx channel power gains. We also proposed a simpler linear rule and saw that it was near-optimal. We derived tight upper bounds for its average SEP and the interference-outage probability. The optimal and linear rules reduced the average SEP by one to two orders of magnitude compared to the existing ASPA rules. We also saw that the estimation errors of the STx-SRx and STx-PRx channels affected the average SEP and interference-outage probability of the optimal rule differently. An interesting avenue for future work is to consider multiple PRxs, antenna subset selection, and imperfect CSI at the STx.

Appendix

A. Proof of Lemma 1

We say that an ASPA rule is feasible if it satisfies the constraints in (4) and (5). By the construction of ϕ^* in (10) and the choice of λ^*, it is clearly a feasible rule. For any feasible rule ϕ, which selects antenna s and transmits with power P_s, define the auxiliary function $L_\phi(\lambda)$ as follows:

$$L_\phi(\lambda) \triangleq \mathbb{E}_{\mathbf{h},\mathbf{g}}\left[\mathsf{S}(P_s, h_s) + \lambda I_{\{P_s g_s > \tau\}}\right]. \tag{54}$$

From the definition of ϕ^* in (10), it is clear that $L_{\phi^*}(\lambda^*) \leq L_\phi(\lambda^*)$. Thus,

$$\begin{aligned}\mathbb{E}_{\mathbf{h},\mathbf{g}}&\left[\mathsf{S}(P_{s^*}, h_{s^*}) + \lambda^* I_{\{P_{s^*} g_{s^*} > \tau\}}\right]\\ &\leq \mathbb{E}_{\mathbf{h},\mathbf{g}}\left[\mathsf{S}(P_s, h_s) + \lambda^* I_{\{P_s g_s > \tau\}}\right].\end{aligned} \tag{55}$$

Using $\mathbb{E}\left[I_{\{a\}}\right] = \Pr(a)$ and rearranging terms, we get

$$\begin{aligned}\mathbb{E}_{\mathbf{h},\mathbf{g}}&\left[\mathsf{S}(P_{s^*}, h_{s^*})\right] \leq \mathbb{E}_{\mathbf{h},\mathbf{g}}\left[\mathsf{S}(P_s, h_s)\right]\\ &+\lambda^*\left(\Pr\left(P_s g_s > \tau\right) - \Pr\left(P_{s^*} g_{s^*} > \tau\right)\right).\end{aligned} \tag{56}$$

Since $\lambda^* > 0$ is chosen such that $\Pr\left(P_{s^*} g_{s^*} > \tau\right) = O_{\max}$, we get

$$\begin{aligned}\mathbb{E}_{\mathbf{h},\mathbf{g}}&\left[\mathsf{S}(P_{s^*}, h_{s^*})\right] \leq \mathbb{E}_{\mathbf{h},\mathbf{g}}\left[\mathsf{S}(P_s, h_s)\right]\\ &+ \lambda^*\left(\Pr\left(P_s g_s > \tau\right) - O_{\max}\right).\end{aligned} \tag{57}$$

Since ϕ is feasible, we must have $\Pr\left(P_s g_s > \tau\right) - O_{\max} \leq 0$. Since $\lambda^* > 0$, the above inequality implies $\mathbb{E}_{\mathbf{h},\mathbf{g}}\left[\mathsf{S}(P_{s^*}, h_{s^*})\right] \leq \mathbb{E}_{\mathbf{h},\mathbf{g}}\left[\mathsf{S}(P_s, h_s)\right]$. Thus, the ASPA rule ϕ^* in (10) is SEP-optimal.

B. Proof of Lemma 2

We consider the $P_{\max} g_k \leq \tau$ and $P_{\max} g_k > \tau$ cases separately.

1) $P_{\max} g_k \leq \tau$: For all $P_k \in [0, P_{\max}]$, we have $I_{\{P_k g_k > \tau\}} = 0$. Since $\mathsf{S}(P_k, h_k)$ is a monotonically decreasing function of P_k, the minimum net cost is obtained by setting $P_k = P_{\max}$.

2) $P_{\max} g_k > \tau$: We consider $P_k \in [0, \tau/g_k]$ and $P_k \in (\tau/g_k, P_{\max}]$ cases separately. For $P_k \in [0, \tau/g_k]$, we have $I_{\{P_k g_k > \tau\}} = 0$. Thus, from (11), $\mathsf{NC}_k = \mathsf{S}(P_k, h_k)$. It takes the smallest value at $P_k = \tau/g_k$. On the other hand, for $P_k \in (\tau/g_k, P_{\max}]$, we have $I_{\{P_k g_k > \tau\}} = 1$. Thus, $\mathsf{NC}_k = \mathsf{S}\left(P_{\max}, h_k\right) + \lambda$. It takes the smallest value at $P_k = P_{\max}$. Thus, the value of P_k that minimizes NC_k can be compactly written as

$$P_k = \begin{cases} P_{\max}, & \text{if } \mathsf{S}\left(\frac{\tau}{g_k}, h_k\right) > \mathsf{S}\left(P_{\max}, h_k\right) + \lambda, \\ \frac{\tau}{g_k}, & \text{else.} \end{cases} \tag{58}$$

Combining the above two cases yields (12).

C. Brief Proof of Lemma 3

Let $Y_k \triangleq \mathsf{S}\left(\tau/g_k, h_k\right) - \mathsf{S}\left(P_{\max}, h_k\right)$, for $1 \leq k \leq N_t$. As h_k and g_k have continuous CDFs and are independent, it can be shown that Y_k also has a continuous CDF [33, Chap. 3]. Note that an interference-outage happens only when $Y_{s^*} > \lambda$. This is because, from (12), $P_{s^*} g_{s^*}$ is greater than τ only in this case. Thus, the interference-outage probability O_λ of ϕ^* is given by

$$O_\lambda = \Pr\left(Y_{s^*} > \lambda\right). \tag{59}$$

We now show that O_λ is a monotonically decreasing and continuous function of λ. Then, by the intermediate value theorem, it follows that a unique $\lambda^* \in (0, c_1)$ exists such that $O_\lambda = O_{\max}$.

1) Monotonicity of O_λ: For $\lambda = 0$, ϕ^* reduces to the UC rule. Hence, $O_\lambda = O_u(\tau) > O_{\max}$. For $0 < \lambda < c_1$, from (59), we see that O_λ decreases as λ increases. At $\lambda = c_1$, $O_\lambda = 0$ because $Y_{s^*} \leq c_1$. Thus, O_λ monotonically decreases from $O_u(\tau)$ to 0 as λ increases from 0 to c_1.

2) Continuity of O_λ: In order to explicitly show the dependence on λ, we denote the antenna selected by ϕ^* as s_λ^* in the rest of this proof. From (59), we have

$$O_\lambda = \sum_{i=1}^{N_t} \Pr\left(s_\lambda^* = i, Y_i > \lambda\right) = N_t \Pr\left(s_\lambda^* = 1, Y_1 > \lambda\right). \tag{60}$$

In order to prove that O_λ is a continuous function of λ, we need to show that $|O_\lambda - O_{\lambda+\epsilon}| = \mathcal{O}(\epsilon)$, for an arbitrary, small ϵ. From (60), we get $|O_\lambda - O_{\lambda+\epsilon}| = N_t |\Pr(A) - \Pr(B)|$, where $A \triangleq \{s_\lambda^* = 1, Y_1 > \lambda\}$ and $B \triangleq \{s_{\lambda+\epsilon}^* = 1, Y_1 > \lambda + \epsilon\}$. By writing $\Pr(A) = \Pr(A \cap B^c) + \Pr(A \cap B)$ and $\Pr(B) = \Pr(A^c \cap B) + \Pr(A \cap B)$, we get

$$\begin{aligned}|O_\lambda - O_{\lambda+\epsilon}| &= N_t |\Pr(A \cap B^c) - \Pr(A^c \cap B)|,\\ &\leq N_t\left[\Pr(A \cap B^c) + \Pr(A^c \cap B)\right].\end{aligned} \tag{61}$$

Without loss of generality, let $\epsilon > 0$. From the definitions of A and B, we get $A \cap B^c = \{s_\lambda^* = 1, Y_1 > \lambda\} \cap \{(s_{\lambda+\epsilon}^* \neq 1) \cup (Y_1 \leq \lambda + \epsilon)\}$. Applying the union bound, we get

$$\begin{aligned}\Pr(A \cap B^c) &\leq \Pr\left(s_\lambda^* = 1, Y_1 > \lambda, Y_1 \leq \lambda + \epsilon\right)\\ &+\Pr\left(s_\lambda^* = 1, Y_1 > \lambda, s_{\lambda+\epsilon}^* \neq 1\right).\end{aligned} \tag{62}$$

The first term in (62) is less than or equal to $\Pr(\lambda < Y_1 \leq \lambda + \epsilon)$. It is $\mathcal{O}(\epsilon)$ for $\epsilon > 0$ because Y_1

is a continuous RV. Similarly, substituting the conditions from (10) under which $s_{\lambda}^* = 1$ and $s_{\lambda+\epsilon}^* \neq 1$, we can show that the second term in (62) is also $\mathcal{O}(\epsilon)$. Combining these two, we get $\Pr(A \cap B^c) = \mathcal{O}(\epsilon)$. Similarly, we can show that $\Pr(A^c \cap B) = \mathcal{O}(\epsilon)$. The details are omitted due to space constraints. Substituting these in (61), we get $|O_\lambda - O_{\lambda+\epsilon}| = \mathcal{O}(\epsilon)$.

D. Proof of Result 1

As the region $\widehat{\mathcal{I}}_k$ is obtained by dropping the positive term $\mathsf{S}(P_{\max}, h_k)$, it follows that $\mathcal{I}_k \subset \widehat{\mathcal{I}}_k$. This is illustrated in Figure 2b. Thus, when $P_{\max} g_k > \tau$, the linear rule transmits with power $P_{\max}$ more often than the optimal rule. Since the SEP monotonically decreases as the transmit power increases, the SEP of the linear rule is lower than that of the optimal rule.

E. Proof of Lemma 4 About $\Pr\left(s = 1, \widehat{U}_1 | h_1\right)$

Among the $(N_t - 1)$ antennas $2, \ldots, N_t$, let j, k, and n be the number of antennas in the OCPP, OCPC, and OI regions, respectively. There are $(N_t - 1)!/(j!k!n!)$ possible combinations, which by symmetry are equally likely. Consider one such event

$$F_{jkn} = \{\widehat{U}_2, \ldots, \widehat{U}_{j+1}, \widehat{C}_{j+2}, \ldots, \widehat{C}_{j+k+1}, \widehat{I}_{j+k+2}, \ldots, \widehat{I}_{N_t}\}, \tag{63}$$

in which antennas $2, \ldots, j+1$, are in the OCPP region, antennas $j+2, \ldots, j+k+1$ are in the OCPC region, and antennas $j+k+2, \ldots, N_t$ are in the OI region. Hence,

$$\begin{aligned} &\Pr\left(s = 1, \widehat{U}_1 | h_1\right) \\ &\quad = \sum_{\substack{j \geq 0, k \geq 0, n \geq 0, \\ j+k+n = N_t - 1}} \frac{(N_t - 1)!}{j!k!n!} \Pr\left(s = 1, \widehat{U}_1, F_{jkn} | h_1\right). \end{aligned} \tag{64}$$

From (18) and (19), we get $\widehat{\mathsf{NC}}_i = \mathsf{S}(P_{\max}, h_i)$, for $i \in \{1, \ldots, j+1\}$, $\widehat{\mathsf{NC}}_i = \mathsf{S}(\tau/g_i, h_i)$, for $i \in \{j+2, \ldots, j+k+1\}$, and $\widehat{\mathsf{NC}}_i = \mathsf{S}(P_{\max}, h_i) + \lambda$, for $i \in \{j+k+2, \ldots, N_t\}$. Therefore, antenna 1 is selected when $h_i < h_1$, for $2 \leq i \leq j+1$, $(\tau h_i / g_i) < P_{\max} h_1$, for $j+2 \leq i \leq j+k+1$, and $\mathsf{S}(P_{\max}, h_i) + \lambda > \mathsf{S}(P_{\max}, h_1)$, for $j+k+2 \leq i \leq N_t$. Hence,

$$\begin{aligned} &\Pr\left(s = 1, \widehat{U}_1, F_{jkn} | h_1\right) \\ &\quad = \Pr\Bigg(\widehat{U}_1, h_2 < h_1, \widehat{U}_2, \ldots, h_{j+1} < h_1, \widehat{U}_{j+1}, \\ &\qquad \frac{\tau h_{j+2}}{g_{j+2}} < P_{\max} h_1, \widehat{C}_{j+2}, \\ &\qquad \ldots, \frac{\tau h_{j+k+1}}{g_{j+k+1}} < P_{\max} h_1, \widehat{C}_{j+k+1}, \\ &\qquad \mathsf{S}(P_{\max}, h_{j+k+2}) + \lambda > \mathsf{S}(P_{\max}, h_1), \widehat{I}_{j+k+2}, \\ &\qquad \ldots, \mathsf{S}(P_{\max}, h_{N_t}) + \lambda > \mathsf{S}(P_{\max}, h_1), \widehat{I}_{N_t}\Bigg). \end{aligned} \tag{65}$$

Using the definitions of the three regions in (16a), (16b), and (16c), we get

$$\begin{aligned} \Pr\left(s = 1, \widehat{U}_1, F_{jkn} | h_1\right) &= \Pr\left(\widehat{U}_1\right) [T_{\mathrm{uu}}(h_1)]^j \\ &\quad \times [T_{\mathrm{uc}}(h_1)]^k [T_{\mathrm{ui}}(h_1)]^n, \end{aligned} \tag{66}$$

where the terms $T_{\mathrm{uu}}(h_1)$, $T_{\mathrm{uc}}(h_1)$, and $T_{\mathrm{ui}}(h_1)$ are defined in the lemma statement. From (9) and (16a), we get $\Pr\left(\widehat{U}_1\right) = \Pr(P_{\max} g_1 \leq \tau) = 1 - O_u(\tau)$. Substituting (66) in (64) and simplifying further yields (27).

F. Proof of Lemma 5 About T_{OCPP}

In (24), we first upper bound $\Pr\left(s = 1, \widehat{U}_1 | h_1\right)$, which is given in (27), by evaluating or bounding the terms $T_{\mathrm{uu}}(h_1)$, $T_{\mathrm{uc}}(h_1)$, and $T_{\mathrm{ui}}(h_1)$ that it is composed of.

i) *$T_{uu}(h_1)$:* As h_2 and g_2 are independent RVs, from (9), we get $T_{\mathrm{uu}}(h_1) = F_h(h_1)(1 - O_u(\tau))$.

ii) *$T_{uc}(h_1)$:* For $(\tau/(h_1 P_{\max})) > m$, we get

$$T_{\mathrm{uc}}(h_1) = \Pr\left(g_2 > \frac{\tau}{h_1 P_{\max}} h_2, P_{\max} g_2 > \tau, g_2 \leq m h_2\right) = 0.$$

For $(\tau/(h_1 P_{\max})) \leq m$, we have $T_{\mathrm{uc}}(h_1) \leq \Pr\left(\widehat{C}_2\right)$.

iii) *$T_{ui}(h_1)$:* Rearranging terms, we get

$$T_{\mathrm{ui}}(h_1) = \Pr\left(\mathsf{S}(P_{\max}, h_2) > \mathsf{S}(P_{\max}, h_1) - \lambda, \widehat{I}_2\right). \tag{67}$$

For $h_1 > \beta_m$, we have $\mathsf{S}(P_{\max}, h_1) - \lambda < 0$. This implies that the inequality $\mathsf{S}(P_{\max}, h_2) \geq 0 > \mathsf{S}(P_{\max}, h_1) - \lambda$ is always true. Hence, $T_{\mathrm{ui}}(h_1) = \Pr(P_{\max} g_2 > \tau, g_2 > m h_2)$. For $h_1 \leq \beta_m$, we have

$$\begin{aligned} T_{\mathrm{ui}}(h_1) &\leq \Pr\left(\mathsf{S}(P_{\max}, h_2) > \mathsf{S}(P_{\max}, h_1) - \lambda, P_{\max} g_2 > \tau\right), \\ &= \Pr\left(h_2 < \omega(h_1), P_{\max} g_2 > \tau\right), \end{aligned} \tag{68}$$

where $\omega(h_1)$ is defined in the lemma statement. Here, (68) follows by substituting the SEP expression in (1) and then rearranging terms.

From above, for $h_1 \leq \beta_m$, we get $T_{\mathrm{uc}}(h_1) + T_{\mathrm{ui}}(h_1) \leq O_u(\tau) F_h(\omega(h_1))$. Similarly, for $h_1 > \beta_m$, we see that $T_{\mathrm{uc}}(h_1) + T_{\mathrm{ui}}(h_1) \leq \Pr(P_{\max} g_2 > \tau, g_2 \leq m h_2) + \Pr(P_{\max} g_2 > \tau, g_2 > m h_2) = O_u(\tau)$. Substituting these inequalities along with the expression for $T_{\mathrm{uu}}(h_1)$ in (27) yields an upper bound for $\Pr\left(s = 1, \widehat{U}_1 | h_1\right)$. Substituting this in (24) and averaging over h_1 yields (28).

G. Proof of Lemma 6 About T_{OCPC}

In (25), we first upper bound $\Pr\left(s = 1, \widehat{C}_1 | h_1, g_1\right)$, which is given in (29). It is non-zero only when $(h_1, g_1) \in \{P_{\max} g_1 > \tau, g_1 \leq m h_1\}$. Thus, we need to simplify the terms $T_{\mathrm{cu}}(h_1, g_1)$, $T_{\mathrm{cc}}(h_1, g_1)$, and $T_{\mathrm{ci}}(h_1, g_1)$ only when (h_1, g_1) lies in this region.

The first term $T_{\mathrm{cu}}(h_1, g_1)$ in (30) simplifies to $F_h(\tau h_1/(P_{\max} g_1))(1 - O_u(\tau))$ since h_2 and g_2 are independent RVs. Rearranging the terms in the expression for $T_{\mathrm{ci}}(h_1, g_1)$ in (32) yields

$$T_{\mathrm{ci}}(h_1, g_1) = \Pr\left(\mathsf{S}(P_{\max}, h_2) > \mathsf{S}(\tau/g_1, h_1) - \lambda, \widehat{I}_2\right). \tag{69}$$

From the definition of m in (17), we have $\mathsf{S}(\tau/g_1, h_1) - \lambda \leq 0$ when $g_1 \leq m h_1$. Since $\mathsf{S}(P_{\max}, h_2) \geq 0$, we get $T_{\text{ci}}(h_1, g_1) = \Pr(P_{\max} g_2 > \tau, g_2 > m h_2)$. Combining this with $T_{\text{cc}}(h_1, g_1)$ in (31), we get $T_{\text{cc}}(h_1, g_1) + T_{\text{ci}}(h_1, g_1) = \Pr((h_2/g_2) < (h_1/g_1), P_{\max} g_2 > \tau)$. Writing this in terms of the fading distributions and substituting it in (29) yields a closed-form expression for $\Pr\left(s = 1, \widehat{C}_1 | h_1, g_1\right)$. Substituting this in (25) and averaging over h_1 and g_1 yields (33).

H. Proof of Lemma 7 About T_{OI}

We first upper bound $\Pr\left(s = 1, \widehat{I}_1 | h_1\right)$, which is given in (34), by evaluating or bounding the terms $\Pr\left(\widehat{I}_1 | h_1\right)$, $T_{\text{iu}}(h_1)$, $T_{\text{ic}}(h_1)$, and $T_{\text{ii}}(h_1)$.

i) $\Pr\left(\widehat{I}_1 | h_1\right)$: For $h_1 > \beta_m$, $\Pr(P_{\max} g_1 > \tau, g_1 > m h_1 | h_1)$ is equal to $\Pr(g_1 > m h_1 | h_1) = F_g^c(m h_1)$. Else, $\Pr(P_{\max} g_1 > \tau, g_1 > m h_1 | h_1) = \Pr(P_{\max} g_1 > \tau) = O_u(\tau)$.

ii) $T_{\text{iu}}(h_1)$: Since the RVs h_2 and g_2 are independent, it follows from (35) that

$$T_{\text{iu}}(h_1) = (1 - O_u(\tau)) \Pr(\mathsf{S}(P_{\max}, h_2) > \mathsf{S}(P_{\max}, h_1) + \lambda). \tag{70}$$

For $h_1 \leq \beta_m$, we can upper bound $T_{\text{iu}}(h_1)$ by dropping λ to get

$$\begin{aligned} T_{\text{iu}}(h_1) &\leq (1 - O_u(\tau)) \Pr(\mathsf{S}(P_{\max}, h_2) > \mathsf{S}(P_{\max}, h_1)), \\ &= (1 - O_u(\tau)) \Pr(h_2 < h_1). \end{aligned} \tag{71}$$

For $h_1 > \beta_m$, we upper bound $T_{\text{iu}}(h_1)$ in (70) by dropping $\mathsf{S}(P_{\max}, h_1)$, which yields

$$\begin{aligned} T_{\text{iu}}(h_1) &\leq (1 - O_u(\tau)) \Pr(\mathsf{S}(P_{\max}, h_2) > \lambda), \\ &= (1 - O_u(\tau)) F_h(\beta_m). \end{aligned} \tag{72}$$

iii) $T_{\text{ic}}(h_1)$: Using the definition of m in (17), we see that the inequality $g_2 \leq m h_2$ is equivalent to $\mathsf{S}(\tau/g_2, h_2) \leq \lambda$. Substituting this in (36), we get $T_{\text{ic}}(h_1) = 0$ because $\mathsf{S}(P_{\max}, h_1) \geq 0$.

iv) $T_{\text{ii}}(h_1)$: Here, for $h_1 \leq \beta_m$, the event $\{h_2 < h_1, P_{\max} g_2 > \tau, g_2 > m h_2\}$ is the same as $\{h_2 < h_1, P_{\max} g_2 > \tau\}$. Hence, from (37), we get $T_{\text{ii}}(h_1) = \Pr(h_2 < h_1, P_{\max} g_2 > \tau) = O_u(\tau) F_h(h_1)$. For $h_1 > \beta_m$, we can write $T_{\text{ii}}(h_1)$ as

$$\begin{aligned} T_{\text{ii}}(h_1) &= \Pr(0 < h_2 \leq \beta_m, P_{\max} g_2 > \tau) \\ &\quad + \Pr(\beta_m < h_2 < h_1, g_2 > m h_2), && (73) \\ &= O_u(\tau) F_h(\beta_m) + \int_{\beta_m}^{h_1} F_g^c(mx) f_h(x)\, dx, && (74) \\ &\leq O_u(\tau) F_h(\beta_m) + \int_{\beta_m}^{\infty} F_g^c(mx) f_h(x)\, dx. && (75) \end{aligned}$$

Substituting the above expressions in (34) gives an upper bound for $\Pr\left(s = 1, \widehat{I}_1 | h_1\right)$. Substituting this bound in (26) and averaging over h_1 yields (38).

I. Brief Proof of Result 2

An interference-outage happens only when an antenna in the OI region is selected. Thus, $O_\lambda = \Pr\left(\widehat{I}_s\right) = N_t \Pr\left(s = 1, \widehat{I}_1\right) = N_t \mathbb{E}_{h_1}\left[\Pr\left(s = 1, \widehat{I}_1 | h_1\right)\right]$. The simplified expression for $\Pr\left(s = 1, \widehat{I}_1 | h_1\right)$ is given in (34). The terms in it are derived in Appendix H.

For $h_1 \leq \beta_m$, we substitute the upper bound for $T_{\text{iu}}(h_1)$ from (71), $T_{\text{ic}}(h_1) = 0$, and $T_{\text{ii}}(h_1) = O_u(\tau) F_h(h_1)$ in (34). This yields $\Pr\left(s = 1, \widehat{I}_1 | h_1\right) \leq O_u(\tau) [F_h(h_1)]^{N_t - 1}$. Similarly, for $h_1 > \beta_m$, we substitute the upper bound for $T_{\text{iu}}(h_1)$ from (72), $T_{\text{ic}}(h_1) = 0$, and the exact expression of $T_{\text{ii}}(h_1)$ from (74) in (34). This yields

$$\Pr\left(s = 1, \widehat{I}_1 | h_1\right) \leq F_g^c(m h_1) \left[F_h(\beta_m) + \int_{\beta_m}^{h_1} F_g^c(mx) f_h(x)\, dx\right]^{N_t - 1}. \tag{76}$$

Combining these two bounds yields an upper bound for $\Pr\left(s = 1, \widehat{I}_1 | h_1\right)$. Substituting this in $N_t \mathbb{E}_{h_1}\left[\Pr\left(s = 1, \widehat{I}_1 | h_1\right)\right]$ and averaging over h_1 yields (45).

References

[1] R. Sarvendranath and N. B. Mehta, "Optimal joint antenna selection and power adaptation for underlay spectrum sharing," in *Proc. Globecom*, Dec. 2019.

[2] W. Zhang, C.-X. Wang, X. Ge, and Y. Chen, "Enhanced 5G cognitive radio networks based on spectrum sharing and spectrum aggregation," *IEEE Trans. Commun.*, vol. 66, no. 12, pp. 6304–6316, Dec. 2018.

[3] A. Garcia-Rodriguez, L. Galati-Giordano, M. Kasslin, and K. Doppler, "IEEE 802.11be extremely high throughput: The next generation of Wi-Fi technology beyond 802.11ax," Feb. 2019, *arXiv:1902.04320*. [Online]. Available: https://arxiv.org/pdf/1902.04320.pdf

[4] *Amendment of the Commission's Rules With Regard to Commercial Operations in the 3550–3650 MHz Band*, document FCC-15-47, FCC, Washington, DC, USA, Feb. 2015.

[5] *Unlicensed Use of the 6 GHz Band; Expanding Flexible Use in Mid-Band Spectrum Between 3.7 and 24 GHz* document FCC-18-147, FCC, Washington, DC, USA, Oct. 2018.

[6] N. N. Krishnan, R. Kumbhkar, N. B. Mandayam, I. Seskar, and S. Kompella, "Coexistence of radar and communication systems in CBRS Bands through downlink power control," in *Proc. IEEE Mil. Commun. Conf. (MILCOM)*, Oct. 2017, pp. 713–718.

[7] P. K. Sangdeh, H. Pirayesh, H. Zeng, and H. Li, "A practical underlay spectrum sharing scheme for cognitive radio networks," in *Proc. INFOCOM*, Apr./May 2019, pp. 2521–2529.

[8] M. Hanif, H.-C. Yang, and M.-S. Alouini, "Transmit antenna selection for power adaptive underlay cognitive radio with instantaneous interference constraint," *IEEE Trans. Commun.*, vol. 65, no. 6, pp. 2357–2367, Jun. 2017.

[9] C. G. Tsinos, S. Chatzinotas, and B. Ottersten, "Hybrid analog-digital transceiver designs for multi-user MIMO mmwave cognitive radio systems," *IEEE Trans. Cogn. Commun. Netw.*, to be published.

[10] A. Afana, I. A. Mahady, and S. Ikki, "Quadrature spatial modulation in MIMO cognitive radio systems with imperfect channel estimation and limited feedback," *IEEE Trans. Commun.*, vol. 65, no. 3, pp. 981–991, Mar. 2017.

[11] X. Li, N. Zhao, Y. Sun, and F. R. Yu, "Interference alignment based on antenna selection with imperfect channel state information in cognitive radio networks," *IEEE Trans. Veh. Technol.*, vol. 65, no. 7, pp. 5497–5511, Jul. 2016.

[12] T. Y. Elganimi, M. S. Alshawish, and M. M. Abdalla, "Enhanced transmit antenna selection using OSTBC scheme with SVD-based hybrid precoding for 5G millimeter-wave communications," in *Proc. ICEEE*, Apr. 2019, pp. 153–157.
[13] Y. He, S. Atapattu, C. Tellambura, and J. S. Evans, "Opportunistic group antenna selection in spatial modulation systems," *IEEE Trans. Commun.*, vol. 66, no. 11, pp. 5317–5331, Nov. 2018.
[14] A. F. Molisch and M. Z. Win, "MIMO systems with antenna selection," *IEEE Commun. Mag.*, vol. 5, no. 1, pp. 46–56, Mar. 2004.
[15] Z. El-Moutaouakkil, K. Tourki, S. Saoudi, and H. Yanikomeroglu, "Optimal TAS for cross-interference mitigation in cognitive MIMO MRC systems," in *Proc. IWCMC*, Jun. 2019, pp. 2058–2063.
[16] F. A. Khan, K. Tourki, M.-S. Alouini, and K. A. Qaraqe, "Performance analysis of a power limited spectrum sharing system with TAS/MRC," *IEEE Trans. Signal Process.*, vol. 62, no. 4, pp. 954–967, Feb. 2014.
[17] H. Y. Kong and Asaduzzaman, "On the outage behavior of interference temperature limited CR-MISO channel," *J. Commun. Netw.*, vol. 13, no. 5, pp. 456–462, Oct. 2011.
[18] K. Tourki, F. A. Khan, K. A. Qaraqe, H.-C. Yang, and M.-S. Alouini, "Exact performance analysis of MIMO cognitive radio systems using transmit antenna selection," *IEEE J. Sel. Areas Commun.*, vol. 32, no. 3, pp. 425–438, Mar. 2014.
[19] Z. Chen, J. Yuan, and B. Vucetic, "Analysis of transmit antenna selection/maximal-ratio combining in Rayleigh fading channels," *IEEE Trans. Veh. Technol.*, vol. 54, no. 4, pp. 1312–1321, Jul. 2005.
[20] R. Sarvendranath and N. B. Mehta, "Antenna selection with power adaptation in interference-constrained cognitive radios," *IEEE Trans. Commun.*, vol. 62, no. 3, pp. 786–796, Mar. 2014.
[21] R. Sarvendranath and N. B. Mehta, "Transmit antenna selection for interference-outage constrained underlay CR," *IEEE Trans. Commun.*, vol. 66, no. 9, pp. 3772–3783, Sep. 2018.
[22] R. Sarvendranath and N. B. Mehta, "Antenna selection in interference-constrained underlay cognitive radios: SEP-optimal rule and performance benchmarking," *IEEE Trans. Commun.*, vol. 61, no. 2, pp. 496–506, Feb. 2013.
[23] S. Kashyap and N. B. Mehta, "SEP-optimal transmit power policy for peak power and interference outage probability constrained underlay cognitive radios," *IEEE Trans. Wireless Commun.*, vol. 12, no. 12, pp. 6371–6381, Dec. 2013.
[24] L. Musavian and S. Aissa, "Fundamental capacity limits of cognitive radio in fading environments with imperfect channel information," *IEEE Trans. Commun.*, vol. 57, no. 11, pp. 3472–3480, Nov. 2009.
[25] T. H. Cormen, C. E. Leiserson, R. L. Rivest, and C. Stein, *Introduction to Algorithms*, 3rd ed. Cambridge, MA, USA: MIT Press, 2009.
[26] A. J. Goldsmith, *Wireless Communications*. Cambridge, U.K.: Cambridge Univ. Press, 2005.
[27] Y. Wang and J. P. Coon, "Difference antenna selection and power allocation for wireless cognitive systems," *IEEE Trans. Commun.*, vol. 59, no. 12, pp. 3494–3503, Dec. 2011.
[28] R. Zhang, F. Gao, and Y.-C. Liang, "Cognitive beamforming made practical: Effective interference channel and learning-throughput tradeoff," *IEEE Trans. Commun.*, vol. 58, no. 2, pp. 706–718, Feb. 2010.
[29] R. Zhang, "On active learning and supervised transmission of spectrum sharing based cognitive radios by exploiting hidden primary radio feedback," *IEEE Trans. Commun.*, vol. 58, no. 10, pp. 2960–2970, Oct. 2010.
[30] L. Zhang *et al.*, "Primary channel gain estimation for spectrum sharing in cognitive radio networks," *IEEE Trans. Commun.*, vol. 65, no. 10, pp. 4152–4162, Oct. 2017.
[31] I. S. Gradshteyn and I. M. Ryzhik, *Table of Integrals, Series, and Products*, 4th ed. New York, NY, USA: Academic, 1980.
[32] S. T. Chung and A. J. Goldsmith, "Degrees of freedom in adaptive modulation: A unified view," *IEEE Trans. Commun.*, vol. 49, no. 9, pp. 1561–1571, Sep. 2001.
[33] H. Royden and P. Fitzpatrick, *Real Analysis*, 4th ed. Upper Saddle River, NJ, USA: Prentice-Hall, 2010.

Rimalapudi Sarvendranath (S'12) received the B.Tech. degree in electrical and electronics engineering from the National Institute of Technology Karnataka, Surathkal, in 2009, and the M.Eng. degree from the Department of Electrical Communication Engineering (ECE), Indian Institute of Science (IISc), Bengaluru, India, in 2012, where he is currently pursuing the Ph.D. degree. From 2009 to 2010, he was a Research Assistant at the Department of Instrumentation, IISc, where he was involved in the development of image processing algorithms. From 2012 to 2016, he was with Broadcom Communications Technologies Pvt. Ltd., Bengaluru, where he worked on the development and implementation of algorithms for LTE and IEEE 802.11ac wireless standards. His research interests include wireless communication, multiple antenna techniques, cognitive radio, and next-generation wireless standards.

Neelesh B. Mehta (S'98–M'01–SM'06–F'19) received the B.Tech. degree in electronics and communications engineering from the Indian Institute of Technology (IIT), Madras, in 1996, and the M.S. and Ph.D. degrees in electrical engineering from the California Institute of Technology, Pasadena, CA, USA, in 1997 and 2001, respectively. He is currently a Professor with the Department of Electrical Communication Engineering, Indian Institute of Science, Bengaluru. He is a Fellow of the Indian National Academy of Engineering (INAE), the National Academy of Sciences India (NASI), and the Indian National Science Academy (INSA). He is a recipient of the Shanti Swarup Bhatnagar Award, Swarnjayanti Fellowship, and the Khosla National Award. He has served on the Board of Governors of the IEEE ComSoc from 2012 to 2015. He has served on the Executive Editorial Committee of IEEE TRANSACTIONS ON WIRELESS COMMUNICATIONS from 2014 to 2017, and as its Chair from 2017 to 2018. He is currently an Editor of IEEE TRANSACTIONS ON COMMUNICATIONS.